Ways to Increase the Length of Single Wall Carbon Nanotubes in a Magnetically Enhanced Arc Discharge

M. Keidar*, I. Levchenko**, A. Shashurin*, A.M. Waas*** and K. Ostrikov**

*The George Washington University, Washington DC 20052, keidar@gwu.edu
** School of Physics, The University of Sydney, Sydney NSW 2006, Australia
*** University of Michigan, Ann Arbor MI

ABSTRACT

Ability to control the properties of single-wall nanotubes produced in the arc discharge is important for many practical applications. Our experiments suggest that the length and purity of single-wall nanotubes significantly increase when the magnetic field is applied to the arc discharge. A model of a single wall carbon nanotube interaction and growth in the thermal plasma was developed which considers several important effects such as anode ablation that supplies the carbon plasma in an anodic arc discharge technique, and the momentum, charge and energy transfer processes between nanotube and plasma. The numerical simulations based on Monte-Carlo technique were performed, which explain an increase of the nanotubes produced in the magnetic field – enhanced arc discharge.

Keywords: single wall carbon nanotubes, arc discharge

1 INTRODUCTION

Despite significant progress in synthesis techniques the nucleation and growth of carbon nanotubes (CNT) are not completely understood. Several techniques were developed for CNT synthesis such as arc discharge, chemical vapor deposition (CVD), and laser ablation [1, 2, 3, 4]. Plasma-enhanced methods of CNT synthesis are one of the most efficient and precise tools of fabrication of the carbon-based nanostructures [5, 6, 7]. Among other techniques, arc discharge is the most practical method of CNT synthesis.

Main feature of the arc discharge is that the carbon nanotubes produced by the arc discharge technique have fewer structural defects than those produced by low temperature techniques probably due to fast growth that prevents defect formation. In addition it was shown that among several method of CNT production, nanotubes produced by the arc discharge have lowest time degradation of emission capability [8] that is very important for field emission applications.

One important issue related to SWNT synthesis is ability to control SWNT properties, such as radius, chirality and length. It was demonstrated that SWNT radius can be controlled by type of the gas in the chamber while gas pressure leads to fairly constant radius (though some tendency of radius increase with the pressure was recently reported [9]). Recently some ideas regarding control of the chirality were suggested [10]. There is tremendous interest in synthesis long SWNT, which will enable new types of MEMS/NEMS systems, such as micro-electric motors and can act as a nanoconducting cable [11]. Recently growth of 4 cm long SWNT was reported [11]. While, in general, arc discharge technique is considered to offer poor flexibility, it is primarily result of limited understanding of the SWNT synthesis mechanism [12]. In this paper we show that the magnetic field provides a considerable increase in the plasma density and electron temperature, and also ensures a significant enlargement of the high-density plasma area. As a result, the longer SWNT of better quality (lower density of the structural defects) can be synthesized.

2 EXPERIMENTAL SET UP

The arc discharge system consists of anode-cathode assembly installed in a stainless steel flanged chamber capped at both ends (Figure 1). A linear drive connected to the bottom of the chamber acts as the anode feed system. Two portholes on the vertical sides of the chamber are connected to a digital pressure transducer and a constant pressure control system. The arc discharge is sustained with a constant power supply, using a LabView feedback program connected to the linear drive of the anode and the power supply generating the arc.

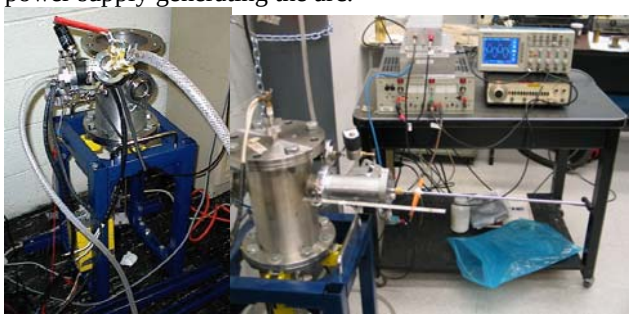

Figure 1: Photo of GWU set up.

The anode is the pure carbon rod while the cathode is stainless steel rod, with the anode being hollow and the cathode being solid. The cathode has a length and diameter of 1.5 in and .5 in, respectively, while the anode has a length of 3 in., and an outer and inner diameter of .25 in and .125 in, respectively. The anode hole is packed with various metal catalysts. Previous quanta sizing and

NSTI-Nanotech 2008, www.nsti.org, ISBN 978-1-4200-8503-7 Vol. 1

microscope examinations of arc-discharge products for equal arc runtime has revealed that the catalyst combination yielding the largest amount of nanotubes was Y-Ni in a 1-4 ratio [13].

The nanotube samples were produced at constant helium pressures ranging from 150 to 750 Torr. The magnetic field was applied to confine the discharge plasma. Samples containing SWNTs were collected after 180 s run of the arc discharge under various conditions – with and without magnetic field. The samples produced were examined under SEM and High Resolution Transmission Electron Microscope (HRTEM). The average ablation rate of the anode was determined by measuring the initial and final anode geometry. From these measurements, the dependency of the anode material consumption on the arc current with and without magnetic field was determined.

3. RESULTS

The current-voltage characteristic of the discharge (without magnetic field) were measured for helium pressures in the range from 150 to 750 Torr, interelectrode gap ~0.5-1 mm and for 2 anode compositions (C:Ni=15:1 and C:Ni:Y=10.4:4:1 wt. % ratio). Typical dependence of arc voltage (U_{arc}) on arc current (I_{arc}) is shown in Fig. 2 (He pressure –750 Torr, anode composition - C:Ni:Y=10.4:4:1). It was found that current-voltage characteristics were slightly depended on the He pressure and anode composition.

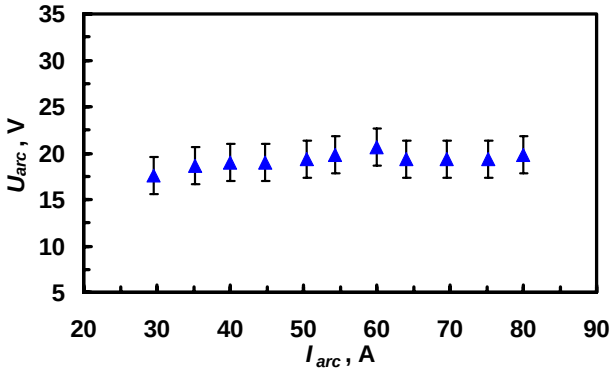

Figure 2: Current-voltage characteristic of the discharge (interelectrode gap ~0.5-1 mm, anode composition - C:Ni:Y=10.4:4:1, He pressure – 750 Torr).

Below we present experimental results related to study of the effect of a magnetic field on SWNT synthesis. Several interesting effects were observed with application of the magnetic field.

The magnetic field strongly confines the plasma causing brighter discharge in smaller zone. We recall here that the application of the magnetic field to the similar discharges usually causes a strong increase in the plasma density [14]. In our previous works we also have demonstrated that the application of magnetic field to the arc discharge leads to the significant change in the cathode and anode erosion rate [15]. It is natural that the carbon deposit produced in the magnetic field – applied discharge is different of those produced without the magnetic field. A detailed analysis and high-resolution TEM images of the carbon deposits have demonstrated that the samples produced in the magnetic field consist mainly of isolated single-wall nanotubes and bundles. In Fig. 3 we show TEM images of various magnification that demonstrate a 6-nm bundle of several SCWNTs (a), bundle and isolated SWCNT (b), as well as a large bundle where the individual nanotubes are perfectly visible (c). The detailed studies, along with the radius measurements, have proved that the nanotubes produced in the magnetic field-assisted discharge are mostly single-walled.

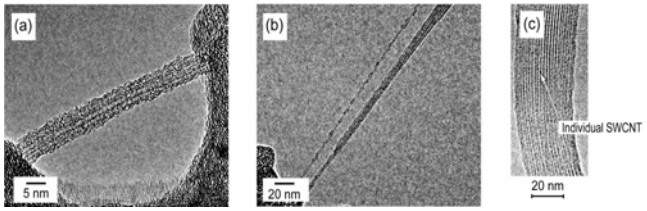

Figure 3: (a) TEM image of the bundle of single-wall carbon nanotubes at high magnification; (b) TEM image of bundle of carbon nanotubes and individual nanotube in parallel the bundle at lower magnification; and (c) TEM image of large bundle of single-wall carbon nanotubes.

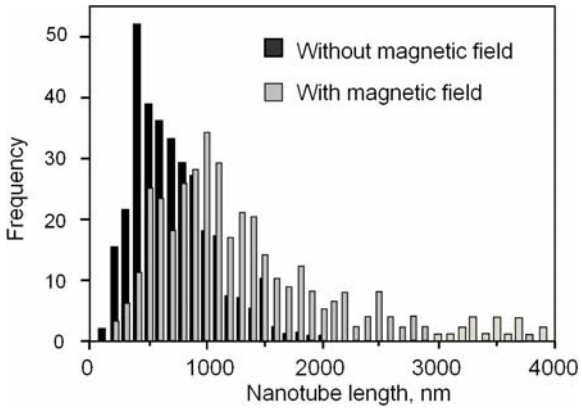

Figure 4: Distribution of SWNT lengths in deposits produced with and without magnetic field. Magnetic field 0.4 T.

We recall again that just the length of the SWCNT are the main our focus; thus we have made a measurement of the nanotubes collected from the deposits produces with and without the magnetic field, and the results obtained are presented in Fig. 4 where we show the distribution of SWCNT length. It can be seen from this graph that the maximum of the distribution of SWCNTs produced without the magnetic field corresponds to 400 nm; for the SWCNTs produced in the magnetic field – enhanced discharge, the

maximum of the length distribution corresponds to 1000 nm, and the deposit contains nanotubes of 4 μm length, with the maximum length of 2 μm found in the deposits produced without magnetic field.

4. SIMULATION

Now we attempt to explain the features of SWNTs growth in the magnetically-enhanced arc discharges. We recall that the application of magnetic field, first of all, strongly increases the plasma density and electron temperature of the discharge. Together with the electric field related effects, this should strongly affect the SWNT growth [16]. We have already shown in our previous works that the ion focusing in nano-scaled systems can play a very important role [17, 18]. Now we present a model that helps to describe a SWNT growth in the dense plasma.

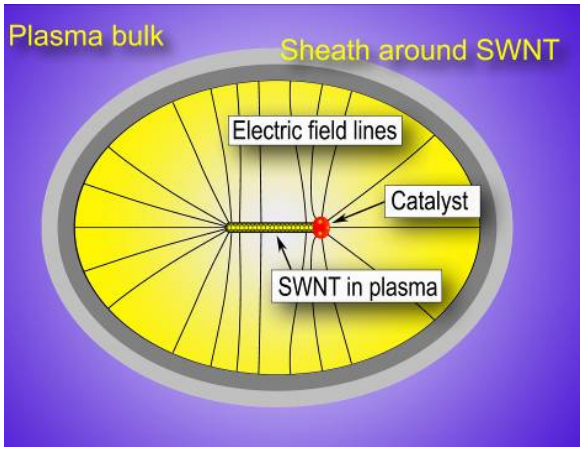

Figure 5: SWNT on metal catalyst particle in plasma. In the practically interesting condition of large sheath ($\Delta << \delta$), the shape of the sheath weakly depend on the SWNT length. Electric field is applied between SWNT/C and plasma bulk border. Carbon ion flux is deposited mainly on SWNT tip and on catalyst particle.

Let us first consider in details the SWNT – plasma interaction. As any object immersed in the plasma, SWNT esquires an electric charge (dependent on plasma density as shown in Fig. 5) and eventually encloses by the plasma – surface sheath which thickness can be estimated as few Debye lengths. The plasma is quasi-neutral outside of the sheath, and the electrical field is close to zero. In the sheath there is a non-compensated electric charge which created an electric field applied to the SWNT surface (Fig. 5).

It was shown that in the process with pure helium the SWNT length reaches several μm [19]; so in our calculations we have assumed the maximum SWNT length of 5 μm. Thus, for the typical plasma density (10^{17} m^{-3} – 10^{18} m^{-3}) and electron temperature (1-5 eV) in the arc discharge we can estimate the sheath thickness in the range of 15 to 50 μm. This estimate shows that the sheath thickness δ well exceeds the SWNT length Δ, and hence the shape of the sheath envelope does not depend significantly on it.

In the vicinity of SWNT, the ion motion is determined by the electrical field between SWNT surface and plasma bulk boundary. The electric field is described by the Poisson equation for the electric potential $\Delta\varphi = \rho_e / \varepsilon_0$, where ρ_e is the density of electrical charge on the sheath. As a boundary condition for the Poisson equation, we assumed the equi-potentiality of the entire SWNT surface (thus we assumed that the SWNT is well conductive): $\varphi(x,r,\alpha)|_{(x,R,\alpha)} = \Psi_{SWNT}$, where Ψ_{SWNT} is the electric potential of the SWNT/C system and *R* is the SWNT radius. With the electric field in the sheath calculated, the ion trajectories can be obtained by integrating the motion equation. More details on the electric field and ion motion calculations on nanostructures can be found elsewhere [20, 21].

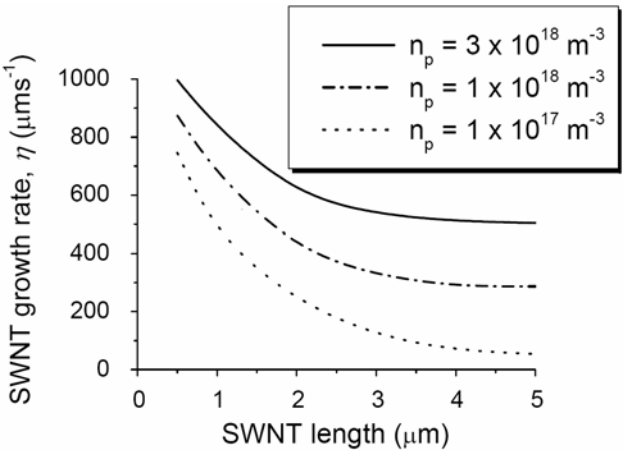

Figure 6. Dependence of SWNT growth rate η on SWNT length with plasma density as a parameter. SWNT diameter 2 nm, catalyst particle diameter is 10 nm. The graph shows strong decrease of SWNT growth rate with the SWNT length.

In this work, we have implemented the following scenario of the SWNT growth in plasma. We assume that the SWNT grows on the partially molten metal catalyst particle supplied to the plasma from ablated electrode (below, we will term the SWNT growing on catalyst particle as SWNT/C system). In the plasma, the metal catalyst particle is a subject to the additional heating and ablation, which reduce the catalyst size, and then condition and molten the external layer creating an external liquid shell. The carbon atom flux gets to the catalyst surface, diffuse through it and eventually incorporate into the SWNT structure. The ion flux at the sheath border – SWNT/C surface supplies carbon atoms to the SWNT/C

NSTI-Nanotech 2008, www.nsti.org, ISBN 978-1-4200-8503-7 Vol. 1

system. Upon recombination, carbon adatoms migrate about the SWNT/C surface and eventually reach the molten catalyst shell or re-evaporate to the plasma bulk. Today, the two main growth scenarios are mostly accepted: the vapor–liquid-solid (VLS) [22, 23] and solid-liquid-solid (SLS) [24]. In despite of the different initial stages, both scenarios involve the carbon atom diffusion in the molten metal of the catalyst particle, and thus the process of the carbon supply to the external catalyst surface is a decisive factor that determines the SWNT growth kinetics. To calculate the carbon supply to the catalyst surface, we implemented a diffusion model which was used for simulation of the diffusion-driven growth of carbon nanostructures on surface [20, 21].

The above described model was used to simulate the SWNT growth on metal catalyst article in plasma. For the ion motion calculations, we used a Monte-Carlo (MC) technique to obtain the ion flux distribution over the SWNT-catalyst surface [25]. The adatom migration in the collisionless approximation about SWNT surface was simulated also by the MC method, and the carbon atoms diffusion in the molten catalyst was calculated by the diffusion equation [25]. The detailed description of the numerical method and boundary conditions can be found elsewhere [25].

The results of the growth rate calculations are shown in Fig. 6, with the plasma density as a parameter. We should point out that the SWNT growth rate strongly decreases with the SWNT length, and increases with the pressure.

REFERENCES

[1] S. Iijima, Nature **354**, 56 (1991).

[2] Z. Huang, J. Xu, Z. Ren, J. Wang, M. Siegal, and P. Provencio, Appl. Phys. Lett. **73**, 3845 (1998).

[3] Y.H. Wang, M.J. Kim, H.W. Shan, C. Kittrell, H. Fan, L.M. Ericson, W.F. Hwang, S. Arepalli, R.H. Hauge, R.E. Smalley, Nano Lett. **5,** 997 (2005).

[4] S. Arepalli, J. Nanosci. Nanotech. **4**, 317 (2004).

[5] C. D. Scott. J. Nanosci. Nanotech. **4**, 377 (2004).

[6] Z. Markovic, B. Todorovic-Markovic, I. Mohai, Z. Farkas, E. Kovats, J. Szepvolgyi, D. Otaševic, P. Scheier, S. Feil, and N. Romcevic. J. Nanosci. Nanotechnol. **7**, 1357 (2007).

[7] K. Ostrikov, Rev. Mod. Phys. **77**, 489 (2005).

[8] Y. Okawa, S. Kitamura, Y.Iseki, 9th Spacecraft charging technology conference, Japan, April 2005.

[9] E.I. Waldorff, A. M. Waas, P.P. Friedmann, and M. Keidar, J. Appl. Phys. **95**, 2749 (2004).

[10] J. Kunstmann, A. Quanddt, and I. Boustani, Nanotechnology **18**, 155703, (2007).

[11] L.X. Zheng, M.J. O'Connell, S.K. Doorn, X.Z. Liao, Y.H. Zhao, E.A. Akhadov, M.A. Hoffbauer, B.J. Roop, Q.X. Jia, R.C. Dye, D.E. Peterson, S.M. Huang, J. Liu, and Y.T. Zhu, Nature Materials **3**, 673 (2004).

[12] M. Keidar, J. Phys. D: Appl. Phys. **40**, 2388-2393 (2007).

[13] M. Keidar, Y. Raitses, A. Knapp, A.M. Waas, Carbon **44**, 1022 (2006).

[14] I. Levchenko, M. Romanov, Surf. Coat. Technol. **184**, 356-360 (2004).

[15] M. Keidar, I. Levchenko, T. Arbel, M. Alexander, A.M. Waas, K. Ostrikov, Appl. Phys. Lett. (in press)

[16] I. Levchenko, K. Ostrikov, M. Keidar and S. Xu. J. Appl. Phys. **98**, 064304 (2005).

[17] I. Levchenko, K. Ostrikov, M. Keidar and S. Xu. Appl. Phys.Lett. **89**, 033109 (2006).

[18] I. Levchenko, K. Ostrikov, E. Tam, Appl. Phys. Lett. **89**, 223108 (2006)

[19] F. Du, Y. Ma, Xin Lv, Yi Huang, F. Li, Y. Chen. Carbon **44**, 1298 (2006).

[20] I. Levchenko, K. Ostrikov. J. Phys. D: Appl. Phys. **40**, 2308-2319 (2007).

[21] I. Levchenko, K. Ostrikov. Phys. Plasmas **14**, 063502 (2007).

[22] J. Gavillet , J. Thibault, O. Stephan, H. Amara , A. Loiseau , C. Bichara et al. J. Nanosci. Nanotechnol. **4**, 346 (2004).

[23] B.B. Wang, Soonil Lee, X.Z. Xu, Seungho Choi, H. Yan, B. Zhang, W. Hao. Appl. Surf. Sci. **236**, 6 (2004).

[24] R. Sen, S. Suzuki, H. Kataura, Y. Achiba. Chem. Phys. Lett. 349, 383 (2001).

[25] I. Levchenko, A. E. Rider, K. Ostrikov, Appl. Phys. Lett. **90**, 193110 (2007).